

SOURCE CHARACTERIZATION FOR AN INLAND LARGE EARTHQUAKE AND NEAR-SOURCE STRONG GROUND MOTION SIMULATION

Katsuhiro KAMAE¹ And Kojiro IRIKURA²

SUMMARY

We simulate strong ground motions during the 1948 Fukui earthquake, Japan with the JMA magnitude 7.1 based on a heterogeneous source model and the hybrid simulation technique. Most of the source models have been assumed to have uniform slip distribution on rectangular fault plane. Such models could generate ground motions only available longer than several seconds, underestimating shorter period motions (< 1 sec) of engineering interest. We assume two source models of reverse (Model-1) and normal (Model-2) types with a heterogeneous slip distribution on fault plane based on the self-similar scaling relationships of seismic moment versus asperity areas and slips by [Somerville et al.,1999]. Simulations have been carried out by the hybrid scheme combined the 3-D Finite Difference Method with the stochastic simulation technique. Large ground motions from both models are spread over the Fukui basin, although peak velocity distributions are slightly difference each other. Areas over 30% collapse ratio during the Fukui earthquake correspond to those with peak velocity over 60 cm/sec for Model-1 and over 80 cm/sec for Model-2. The level of the peak velocity in the areas with more than 30% collapse ratio are estimated to be over 80 cm/sec based on the previous studies by [Moroi et al.,1998] and [Miyakoshi and Hayashi,1998]. From this result and the comparison of pseudo velocity response spectral level with those within the damage belt during the 1995 Hyogo-ken Nanbu earthquake, we conclude that the damage distribution during the Fukui earthquake is well explained by strong ground motions simulated for Model-2 combined the normal fault model by [Kikuchi et al.,1999] with a standardized heterogeneous source model developed by [Somerville et al.,1999]

INTRODUCTION

The studies of the 1994 Northridge earthquake and the 1995 Hyogo-ken Nanbu earthquake showed that it is very important to characterize the heterogeneity on the fault surface of future earthquakes and to model a wave-field in each realistic media in the prediction of near-source strong ground motions. In particular, the combined effects of the source process and the wave propagation path (basin edge effect) played a key role in generating destructive ground motions in the latter earthquake. Recently, [Somerville et al.,1999] succeeded in characterizing the slip models for enough crustal earthquakes derived from longer period ground motions. They finally found that slip models and the asperities on them scale in a self-similar manner with increasing seismic moment. On the other hand, there are some preliminary evidences that slip models derived from longer-period ground motion recordings are relevant for simulation of high-frequency ground motions of engineering interest [e.g.,Kamae and Irikura,1998; Hartzell et al.,1996; Somerville et al,1996; Wald et al.,1988]. In this

¹ Research Reactor Inst, Kyoto University, Kumatori-cho Sennan-gun, Osaka, Japan. E-mail kamae@kuca.rii.kyusho-u.ac.jp

² Disaster Prevention Research Inst, Kyoto University, Gokasho, Uji, Japan. E-mail irikura@egmdpri01.dpri.kyoto-u.ac.jp

study, we examine the capability of the self-similar scaling law derived by [Somerville et al.,1999] from simulating the strong ground motions during the 1948 Fukui earthquake ($M_{jMA}=7.1$), Japan. The reason why we treat the 1948 Fukui earthquake is that this earthquake occurred just beneath the urban district (Fukui city) as same as the 1995 Hyogo-ken Nanbu earthquake and caused serious damage, including more than 3,700 deaths, widely throughout the Fukui basin. So far, to our regret, there are no existing source models available for simulating strong ground motions from the 1948 Fukui earthquake. First of all, we try to construct the heterogeneous source model composed of only asperities (which are defined as regions of large slip on the fault) according to the self-similar scaling law of seismic moment versus asperity areas and slips by [Somerville et al.,1999]. Strong ground motions are simulated by hybrid scheme which is similar to that proposed by [Kamae et al.,1998]. Finally, we verify the validity of our heterogeneous source model and simulation technique by comparing the damage distribution during the 1948 Fukui earthquake and computed maximum velocity and instrumental seismic intensity distributions and so on.

SIMULATION METHODOLOGY

[Kamae et al.,1998] have proposed the hybrid Green's function method (HGF, hereafter) as an extension of the empirical Green's function method (EGF, hereafter). Here, we outline this method. The important aspect is to use the synthetic Green's functions that are calculated based on a hybrid scheme that combines different methods for calculating the low (in general lower than 1 Hz) and high (in general higher than 1 Hz) frequency part of the Green's functions. The low frequency Green's function is calculated by a 3-D Finite Difference method assuming a point source located in the source area and using a velocity model of the irregular geological structure. The high frequency one is calculated using the stochastic simulation technique of [Boore, 1983] under correction of the effect of the local surface layers not included in it. Strong ground motion from a large earthquake are obtained by the summation of the hybrid Green's function synthesized combining both Green's functions in time domain. In this study, we used a slightly different hybrid scheme to improve synthetic long-period ground motion. Fig. 1 shows the flow chart of simulation methodology of strong ground motion using hybrid scheme. The different aspect from HGF is to simulate the long-period ground motion for each subfault divided on the fault plane.

CONSTRUCTION OF HETEROGENEOUS SOURCE MODEL FOR THE 1948 FUKUI EARTHQUAKE

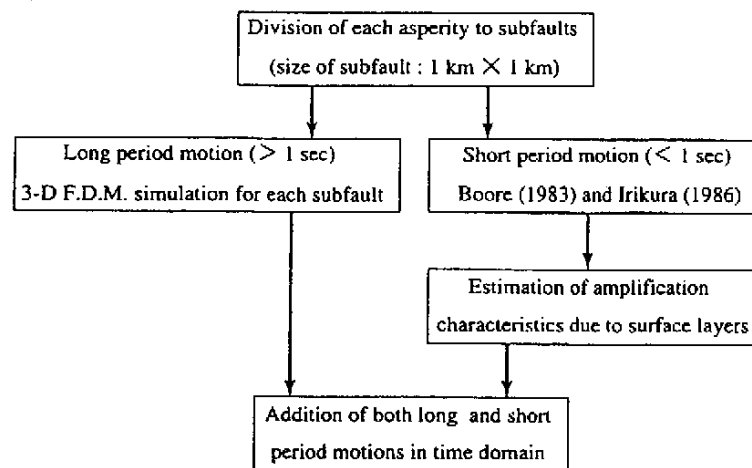


Fig.1: Flow chart of simulation procedure of strong ground motions using a hybrid scheme. The long and short period motions for the hypothetical large earthquake are simulated using 3-D Finite Difference Method considering irregular structure and following the EGF by Irikura (1986) in which small event motions calculated with the stochastic simulation method by Boore (1983) are summed.

[Somerville et al., 1999] analyzed the characteristics of slip models of fifteen crustal earthquakes. They have defined an asperity as a rectangular region in which the slip exceeds, in a specified manner, the slip averaged over the entire fault plane. As a result, they found that the scaling of the fault parameters with seismic moment is reasonably well fit a self-similar model which is convenient to use for strong motion prediction. We showed some relations used in this study below.

The relation between entire rupture area S (km²) and seismic moment M_0 (dyne*cm) is:

$$S=2.23 \times 10^{-15} \times M_0^{2/3} \quad (1)$$

The relation between the area of the largest asperity S_m (km²) and seismic moment M_0 (dyne*cm) is:

$$S_m=3.64 \times 10^{-16} \times M_0^{2/3} \quad (2)$$

The relation between the combined area of asperities S_a (km²) and seismic moment M_0 (dyne*cm) is:

$$S_a=5.00 \times 10^{-16} \times M_0^{2/3} \quad (3)$$

It remains an ambiguity in their definition of asperity area. The effectiveness of the definition should be verified by the forward modeling based on the source model with asperities as [Kamae and Irikura, 1998] have done for the 1995 Hyogo-ken Nanbu earthquake. One of objectives in this study is also to verify such a effectiveness.

The source process of the 1948 Fukui earthquake has been estimated by several researches by the inversion techniques using long-period motion and geodetic data. One of them is a reverse fault model determined from

Table 1: Source parameters for simulating strong ground motions during the 1948 Fukui earthquake. The parameters correspond to map of locations of the main causative fault and two asperities in the fault plane in Fig.3 and the heterogeneous source model with two asperities in Fig.2.

Parameters	Estimates	Comments
Strike · Dip · Rake	(1) 345° · 80° · 26°	Yoshioka (1974)
	(2) 170° · 70° · -10°	Kikuchi et al. (1999)
Seismic Moment (M_0)	2.6×10^{19} (N*m)	* 1
Number of Asperities	2	Kikuchi et al.(1998)
Rupture Area (S)	908 km ²	Somerville et al. (1999)
Combined Area of Asperities (S_a)	204 km ²	Somerville et al. (1999)
Area of Largest Asperity (S_{a2}) (No.2 Asperity)	148 km ² (12km × 12km)	Somerville et al. (1999)
Area of Another Asperity (S_{a1}) (No.1 Asperity)	56 km ² (7km × 8km)	$S_{a1}=S_a-S_{a2}$
Seismic Moment of No.2 Asperity (M_{02})	8.3×10^{18} (N*m)	$M_{02}=M_0 \times S_{a2}/S \times 2.0$
Seismic Moment of No.1 Asperity (M_{01})	3.2×10^{18} (N*m)	$M_{01}=M_0 \times S_{a1}/S \times 2.0$
Stress Drop of No.2 Asperity	113 (bars)	$\Delta\sigma=7/16 \times M_{0a}/r^3$
Stress Drop of No.1 Asperity	186 (bars)	
Average Slip of No.2 Asperity	1.7 (m)	$\mu=3.3 \times 10^{11}$ (dyne/cm ²)
Average Slip of No.1 Asperity	1.7 (m)	
Rise Time	0.6 (sec)	Kamae and Irikura (1998)

* 1 Average of M_0 estimated by Kanamori (1973) and Kikuchi et al. (1999)

the analysis of geodetic data by [Yoshioka, 1974]. Recently, [Kikuchi et al., 1999] reestimated the source process using low gain strong motion data at several observatories of Japan Meteorological Agency and obtained a normal fault model. In this study, we assumed these two source models as Model-1 and Model-2. Heterogeneous slip distribution on fault plane is estimated based on the self-similar scaling relationships represented by equations from (1) to (3). Then we obtained the standardized source model consisting of two asperities to have the average characteristics of asperities for seismic moment of the 1948 Fukui earthquake. Relative locations and rupture times of the asperities on the fault plane are determined following the source model by [Kikuchi et al., 1999]. The maximum asperity corresponding to the second event in their model has an area of $12 \times 12 \text{ km}^2$ and slip of 1.7 m and is located under the most heavily damaged area along the buried fault, known as the Fukui earthquake fault. The smaller asperity corresponding to the first event is located north of the maximum asperity. Rupture was initiated at the northern edge of the smaller asperity, propagated toward south, then broke to start the maximum asperity 7 seconds after the initial rupture. In Table 1 we list the fault parameters for each asperity. The source model consisting of two asperities for Model-1 and Model-2 is shown in Fig 2. Fig.3 shows the Fukui basin and analyzed area. Large solid rectangle in (a) shows the

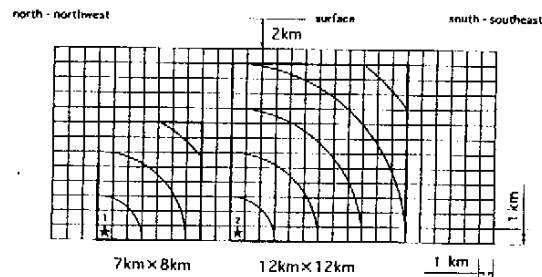


Fig.2: Source model for simulating the strong ground motions from the 1948 Fukui earthquake. Smaller asperity corresponds to No.1 Asperity with an area of $7 \times 8 \text{ km}^2$ and the largest one to No.2 Asperity with $12 \times 12 \text{ km}^2$. Rupture starts from the left bottom at each asperity marked by \star . No.2 Asperity is assumed to break 7 seconds after No.1 according to Kikuchi et al.(1999).

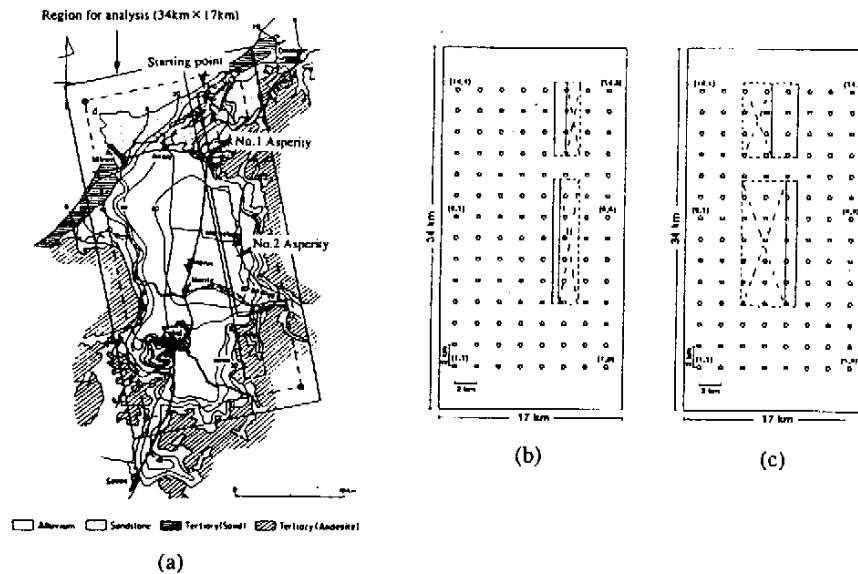


Fig.3: Map of the Fukui basin and analyzed area. Large solid rectangle in (a) shows the analyzed area corresponding to the rectangles in the right two panels, (b) and (c). The broken rectangle in (a) corresponds to areas where peak velocity, acceleration, and instrumental seismic intensity are shown in later figures. The locations of two asperities, No.1 and No.2, in (a) correspond to those for Model-1. Symbols \circ in (b) and (c) show grid points where ground motions are simulated. The two strips indicated with broken X mark in (b) and (c) shows the locations of the two asperities for Model-1 and Model-2, respectively.

analyzed area corresponding to the rectangles in the right panels, (b) and (c). We assumed that the fault surface trace of both models is the same as shown in (b) and (c). The broken rectangle in (a) corresponds to areas where peak velocity, acceleration, and calculated seismic intensity are shown in later figures. Contour map in (a) shows the percentage of collapsed residential wooden houses proposed by the Special Committee of Hokuriku Earthquake in 1951.

MODELING OF UNDERGROUND STRUCTURE

Recently, the underground structure in Fukui basin was explored by refraction survey and boring to investigate the location of the causative fault that generated strong ground motions during the 1948 Fukui earthquake. Moreover, [Yamanaka et al.,1998] and [Wakamatsu and Nobata,1998] proposed a underground structure model from microtremor array measurements. We compiled these informations and estimated a preliminary underground velocity structure such as shown in Fig.4. This model includes a single sedimentary layer (layer A) with shear-wave velocity $V_s=0.6$ km/sec, compressional wave velocity $V_p=2.0$ km/sec, and three background layers (B,C and D). The maximum thickness of the sedimentary layer is about 240 m. Long period ground motions (longer than 1 sec) are simulated by the 3-D Finite Difference Method using this model. Short period ground motions are simulated considering a lower velocity layer with shear-wave velocity $V_s=0.3$ km/sec, compressional wave velocity 1.6 km/sec above A layer. The space distribution of the thickness is assumed based on the H/V characteristics of microtremors by [Wakamatsu and Nobata,1998].

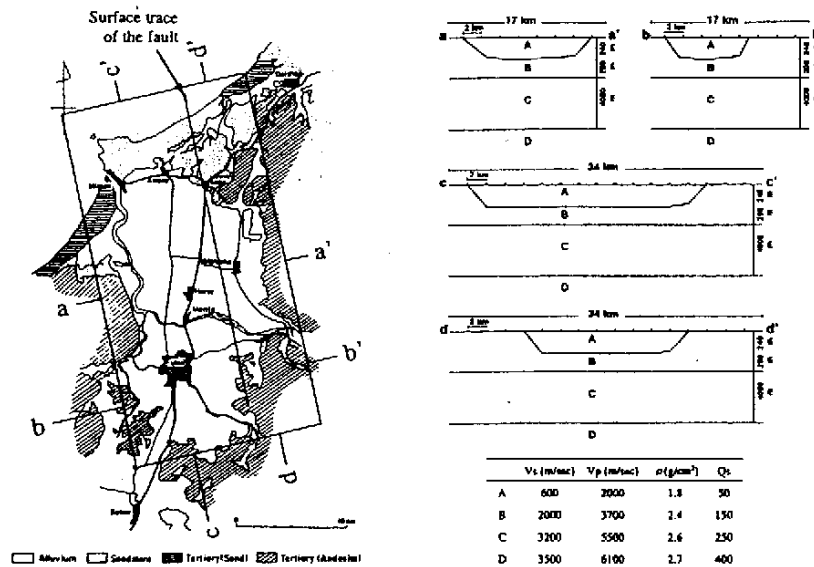


Fig.4: Map of the Fukui basin (left) and cross sections of underground structures (right). The location of the surface fault trace is shown by a solid line in the map. S wave velocity (V_s), P wave velocity (V_p), Density (ρ), and Q factor of S wave in each layer, A,B,C, and D, are shown in the right bottom.

SIMULATION RESULTS

Strong ground motions are simulated at 112 grid points showing by circles in the right two panels in Fig.3 using presented hybrid scheme. Fig.5 and 6 show the contour maps of peak horizontal velocity (vectorial summation of fault normal and parallel components) and instrumental seismic intensity for Model-1 and Model-2, respectively. The presented area in all figures correspond to the broken rectangle shown in Fig.3 (a). Large ground motions from both models, Model-1 and 2, are spread over the Fukui basin, although peak velocity distributions are slightly difference between the two models. In order to conclude which model is better to reproduce the strong ground motions during the 1948 Fukui earthquake, we examine the relation between the level of the synthesized peak velocity in the areas and the observed collapse ratios based on the several studies in the 1995 Hyogo-ken Nanbu earthquake. Roughly speaking, areas over 30% collapse ratio, which is assumed to be the middle of 20% and 40% . because the contour of 30% is not represented in Fig.3 (a).

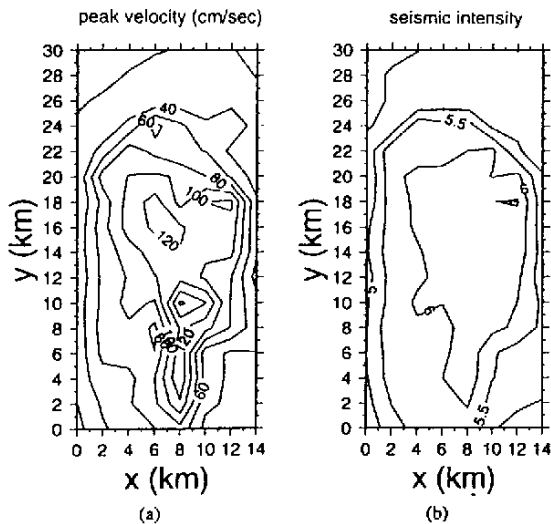


Fig.5: Map showing contours of synthetic peak horizontal velocity (a) (vectorial summation of fault normal and parallel motions) and instrumental seismic intensity (b) for Model-1 (Reversal fault model).

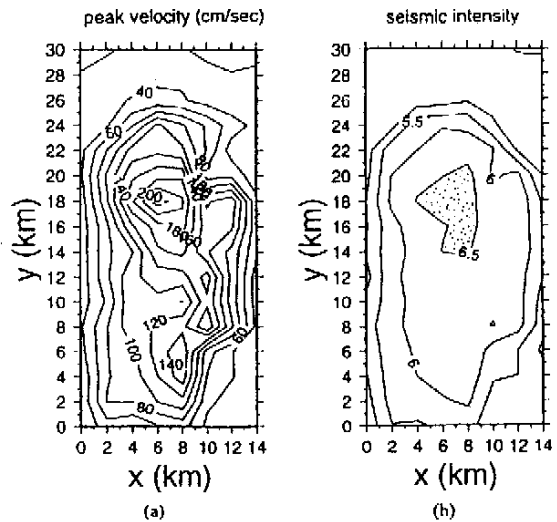


Fig.6: Map showing contours of synthetic peak horizontal velocity (a) (vectorial summation of fault normal and parallel motions) and instrumental seismic intensity (b) for Model-2 (Normal fault model).

correspond to those with peak velocity over 60 cm/sec for Model-1 and over 80 cm/sec for Model-2 from Fig.3(a), Fig.5 and 6. The level of the peak velocity in the areas with more than 30% collapse ratio are estimated to be over 80 cm/sec based on the studies by [Moroi et al.,1998] and [Miyakoshi and Hayashi, 1998]. This result supports that Model-2 is better for the fault model of the 1948 Fukui earthquake. Moreover, as shown in Fig.7, pseudo velocity response spectra in the center of the Fukui basin for Model-2 have almost the same level of the observed one at Takatori (TKT) and the simulated one at Fukuike (FKI) within the damage belt during the 1995 Hyogo-ken Nanbu earthquake by [Kamae and Irikura,1998]. The spectra shown in Fig.7 are calculated from the synthetic waveforms for Model-2 shown in Fig.8. The peak velocity of the corresponding synthetic waveform for the fault parallel component at (9,4) point is over 200 cm/sec (about 220 cm/sec). This estimate is equal to or over the values estimated within the damage belt during the 1995 Hyogo-ken Nanbu earthquake by [Kawase et al.,1996] and [Kamae and Irikura,1998]. Finally, we try to compare the above synthetic results and another ones which are simulated considering the fault slip in the area except for asperities. Then the stress drop in the area except for asperities is assumed to be about 19 bars from the constraint to match the total seismic moment of the 1948 Fukui earthquake. Fig.9 shows the comparison of the distribution of the synthetic peak velocities using two fault models. We can see that both results are almost similar in peak velocity and its distribution. This means that our fault

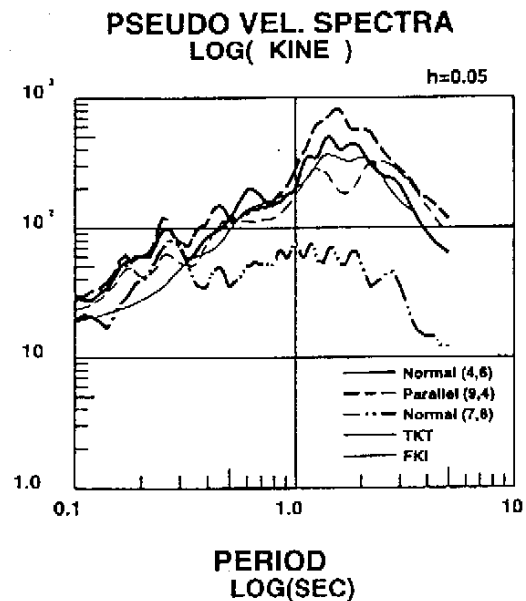


Fig.7: Pseudo velocity response spectra of simulated ground motions on sediments (thick solid line for the fault normal component at grid (4,6) and thick broken line for the fault parallel component at grid (9,4)) and on rock (thick W-dotted chain for the fault normal component at grid (7,8)) for Model-2. For comparison those of the observed motion at Takatori (TKT) and the simulated motion at Fukuike Junior School (FKI) within the damage belt during the 1995 Hyogo-ken Nanbu earthquake are shown with thin solid and broken lines.

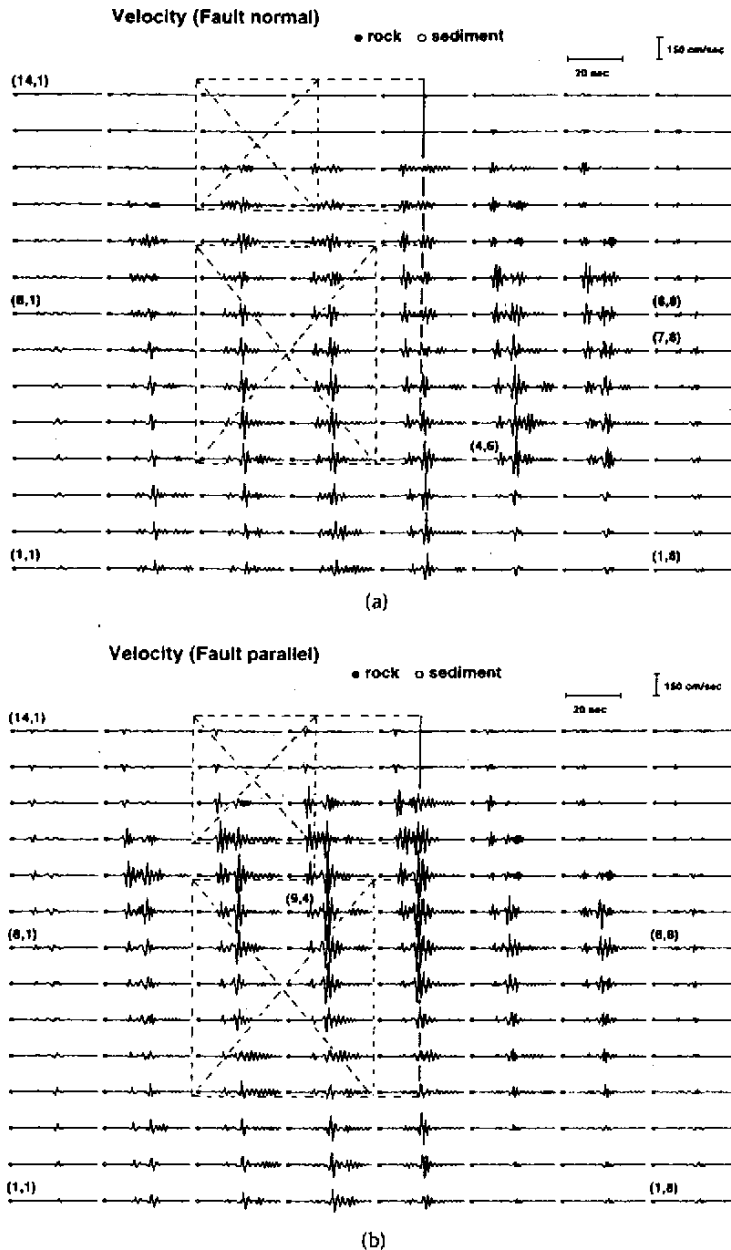


Fig.8: Distribution of simulated velocity ground motions at the grids shown by circles in the right of Fig.3 for Model-2 (Normal fault model). (a) : fault normal component, (b) : fault parallel component, The grid coordinates are indicated by parenthesis at the left-hand of each waveform. Site conditions are classified by ● for rock and ○ for sediment. Amplitude level of each waveform is shown at right-upper with a bar indicating 150 cm/sec.

model considering strong motion generation from only the asperities is useful for simulating strong motions.

CONCLUSIONS

We simulated strong ground motions during the 1948 Fukui earthquake with the JMA magnitude 7.1 based on the heterogeneous source model and the hybrid simulation technique. The heterogeneous source model was constructed based on the self-similar scaling relationships of seismic moment versus asperities areas and slips by [Somerville et al 1999]. We assumed two source models of a reverse fault model (Model-1) determined

by [Yoshioka, 1974] and a normal fault model (Model-2) by [Kikuchi et al., 1999] under the same heterogeneity. The synthetic large ground motions from both models are spread over the Fukui basin because of locating the fault plane just under the basin. From the comparison between the peak velocity in the basin estimated by both models and the damage ratio (the percentage of collapsed residential wooden houses proposed by the Special Committee of Hokuriku Earthquake in 1951) during the 1948 Fukui earthquake, we conclude that Model-2 combined the normal fault model with the standardized heterogeneous source model can be accepted. Such a conclusion suggests that we have a possibility to predict strong ground motions from a future inland large earthquake based on the empirical source modeling with heterogeneity and hybrid simulation technique presented in this study.

REFERENCES

- Boore, D.M. (1983), "Stochastic simulation of high-frequency ground motions based on seismological models of the radiated spectra", *Bull. Seism. Soc. Am.*, 73, pp1865-1894.
- Hartzell, S.H. et al. (1996), "The 1996 Northridge, California earthquake: Investigation of rupture velocity, rise time, and high-frequency radiation", *J. Geophys. Res.*, 101, pp20091-20108.
- Irikura, K. (1986), "Prediction of strong acceleration motion using empirical Green's function", *Proc. 7th Japan Earthq. Eng. Symp.*, pp151-156.
- Kamae, K. and Irikura, K. (1998), "Source model of the 1995 Hyogo-ken Nanbu earthquake and simulation of near-source ground motion", *Bull. Seism. Soc. Am.*, 88, pp400-412.
- Kamae, K., Irikura, K. and Pitarka, A. (1998), "A technique for simulating strong ground motion using hybrid Green's function", *Bull. Seism. Soc. Am.*, 88, pp357-367.
- Kawase, H. et al. (1996), "Ground motion estimation in the Higashinada ward in Kobe during the Hyogo-ken Nanbu earthquake of 1995 based on aftershock records", *J. Struct. Constr. Eng. (Trans. AIJ)*, 476, pp103-112. (in Japanese)
- Kikuchi, M. et al. (1999), "Source parameters of the 1948 Fukui earthquake inferred from low-gain strong-motion records", *Jishin-2*, inprint.
- Miyakoshi, J. and Hayashi, Y. (1998), "Seismic performance of wooden building groups based on building damage data", *The 3rd symp. on earthquake disaster in urban district*, pp315-318.
- Moroi, T. et al. (1998), "Relationship between collapse ratio of wooden houses and JMA seismic intensity from the 1995 Great Hanshin Earthquake", *Abstracts of 1998 Japan Earth and Planetary Science Joint Meeting*, sm-034, p384.
- Somerville, P. et al. (1996), "Implications of the Northridge earthquake for strong ground motions from thrust faults", *Bull. Seism. Soc. Am.*, 86, ppS115-S125.
- Somerville, P. et al. (1999), "Characterizing crustal earthquake slip models for the prediction of strong ground motion", *Seis. Res. Lett.*, 70, pp59-80.
- Wakamatsu, K. and Nobata, A. (1998), "Underground structure of Fukui plain and interpretation on the damage of Fukui earthquake at 1948, Part-1", *Summaries of technical papers of annual meeting in AIJ, B-2*, pp227-228.
- Wald, D.J. et al. (1988), "Simulation of acceleration time histories close to large earthquakes", *Earthquake Engineering and Soil Dynamics II: Recent Advances in Ground Motion Evaluation*, Geotechnical Special Publication 20, J. Lawrence von Thun, ed., pp430-444.
- Yamanaka, H. et al. (1998), "Microtremor array measurements and earthquake observation in the Fukui plain", *Abstracts of 1998 fall meeting in the Seismological Society of Japan*, A15.

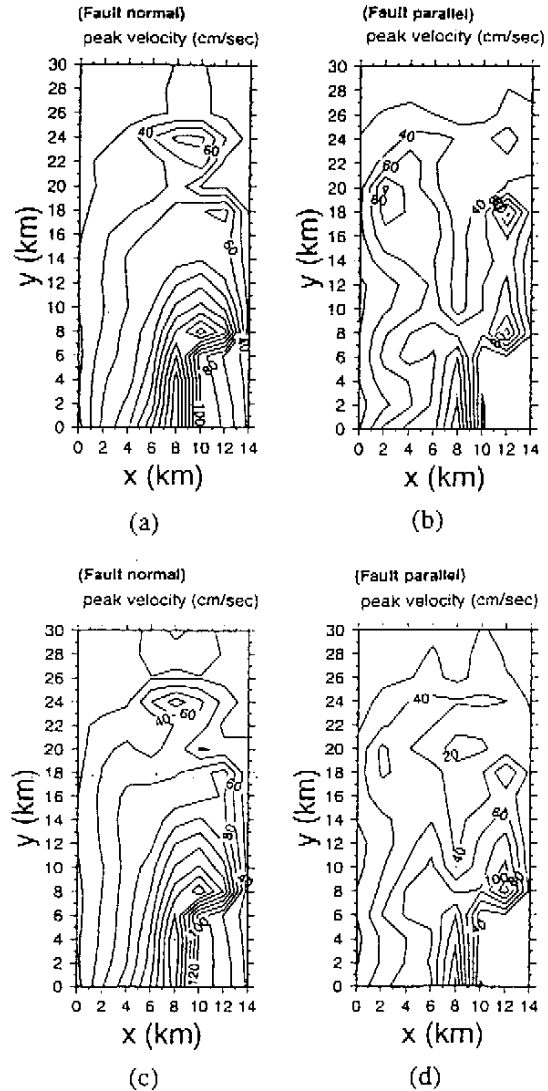


Fig.9: Map showing contours of synthetic peak velocity (a),(b) for Case-1 and (c),(d) for Case-2. Case-1 is the case of assuming that ground motions are generated from only asperities. Case-2 is the case of assuming that ground motions are generated from not only asperities but also background. The both simulations have been done using Model-1 basically.